https://doi.org/10.5194/egusphere-2023-660
Preprint. Discussion started: 2 May 2023

Inferring heavy tails of flood distributions from common discharge dynamics

Hsing-Jui Wang[1], Ralf Merz[1,2], Soohyun Yang[3,4], and Stefano Basso[1,5]

[1]Department of Catchment Hydrology, Helmholtz Centre for Environmental Research – UFZ, Halle (Saale), 06120, Germany,
[2]Institute of Geosciences and Geography, Martin-Luther University Halle-Wittenberg, Halle (Saale), 06120, Germany,
[3]Department of Aquatic Ecosystem Analysis, Helmholtz Centre for Environmental Research – UFZ, Magdeburg, 39114, Germany
[4]Department of Civil and Environmental Engineering, Seoul National University, Seoul, 08826, Republic of Korea
[5]Norwegian Institute for Water Research (NIVA), Oslo, 0579, Norway

Correspondence to: H. –J. Wang (hsing-jui.wang@ufz.de)

Abstract. Floods are often disastrous due to underestimation of the magnitude of rare events. Underestimation commonly happens when the occurrence of floods follow a heavy-tailed distribution, but this behavior is not recognized and thus neglected for flood hazard assessment. In fact, identifying heavy-tailed flood behavior is challenging because of limited data records and the lack of physical support for currently used indices. We address these issues by deriving a new index of heavy-tailed flood behavior from a physically-based description of streamflow dynamics. The proposed index, which is embodied by the hydrograph recession exponent, enables inferring heavy-tailed flood behavior from daily flow records, even of short length. We test the index in a large set of case studies across Germany encompassing a variety of climatic and physiographic settings. Our findings demonstrate that the new index enables reliable identification of cases with either heavy or nonheavy tailed flood behavior from daily flow records. Additionally, the index suitably estimates the severity of tail heaviness and ranks it across cases, achieving robust results even with short data records. The new index addresses the main limitations of currently used metrics, which lack physical support and require long data records to correctly identify tail behaviors, and provides valuable information on the tail behavior of flood distributions and the related flood hazard in river basins using commonly available discharge data.

1 Introduction

Floods remain the leading natural hazards worldwide, which directly threaten the livelihoods of at least one-fifth of the world's population (McDermott, 2022; Rentschler et al., 2022) and have caused enormous economic losses (Bevere and Remondi, 2022). To assess the flood hazards of extreme events, flood frequency analysis is the central and commonly used tool, which is usually achieved by parametrically fitting a selected probability distribution on flow maxima, e.g., the annual maximum flood (Villarini and Smith, 2010), or peak-over-threshold series (Pan et al., 2022). Selecting a suitable distribution that can properly describe (or predict) the extreme events is, however, often challenging due to the notable uncertainties caused by the lack of data in the maxima approach (Papalexiou and Koutsoyiannis, 2013; Hu et al., 2023). The upper-tailed behavior (which

https://doi.org/10.5194/egusphere-2023-660
Preprint. Discussion started: 2 May 2023

we will refer to as 'tail behavior' throughout the paper for simplicity) of the underlying distribution critically determines the accuracy of the extreme events. If a catchment has the potential for heavy-tailed flood behavior but this characteristic is not accounted for in the selection of probability distributions, the probability of extreme floods may be significantly underestimated (Merz et al., 2022). This can lead to disastrous floods and severe damages (Merz et al., 2021). Therefore, correctly identifying the tail behavior of flood distributions is crucial for avoiding potential underestimation of extreme floods. The tail heaviness of an empirical distribution is typically estimated through graphical or statistical methods, although both methods have limitations. Graphical methods, such as log-log plots (Beirlant et al., 2004), generalized Hill ratio plots (Resnick, 2007; El Adlouni et al., 2008), and mean excess functions (Embrechts et al., 1997; Nerantzaki and Papalexiou, 2019), are less objective and efficient for large-scale analyses (Cooke et al., 2014). In contrast, statistical methods, such as parametric metrics that fit distributions to the observed data (Papalexiou et al., 2013; Seckin et al., 2011; Smith et al., 2018; Villarini and Smith, 2010) and non-parametric metrics like the upper tail ratio (Lu et al., 2017; Smith et al., 2018; Villarini et al., 2011; Wang et al., 2022), Gini index (Eliazar and Sokolov, 2010; Rajah et al., 2014), and obesity index (Cooke and Nieboer, 2011; Sartori and Schiavo, 2015), provide a more objective insight into tail behavior. However, obtaining reliable estimates from these methods requires long data records (Papalexiou and Koutsoyiannis, 2013), which can be challenging globally (Lins, 2008) and may cause bias when comparing data across sites with different record lengths (Cunderlik and Burn, 2002; Wietzke et al., 2020). To reduce uncertainty, especially in estimating extremes, it is recommended to analyze ordinary dynamics instead of focusing solely on maximum values (Marani and Ignaccolo, 2015; Mushtaq et al., 2022), and to investigate the underlying factors that contribute to extreme events (Wilson and Toumi, 2005; Tarasova et al., 2020; Merz et al., 2022).

This study aims to investigate whether a suitable descriptor of the tail behavior of flood distributions exists by exploring the intrinsic hydrological dynamics of the flow regime. Currently, widely-used metrics for tail behavior estimation of flood distributions do not incorporate such a physical description, to the best of our knowledge. Using this descriptor as a proxy for estimating heavy-tailed flood behavior, rather than relying solely on statistical analysis of extreme events, we aim to bridge this gap and improve the accuracy and reliability of tail behavior estimation for flood distributions. We begin the analysis with a mechanistic description of hydrological processes. We subsequently distinguish between the key processes generating heavy and nonheavy tailed behavior of flood distributions and propose a physical descriptor for heavy-tailed flood behavior which is based on common streamflow dynamics. We verify its ability to identify heavy-tailed flood behavior and its robustness in datasets with decreasing lengths through numerous case studies across Germany, encompassing various climate and physiographic characteristics. This confirms the practical transferability and stability of the descriptor.

2 Identifying tail behavior from hydrological dynamics

We describe key hydrologic processes occurring at the catchment scale and the resulting probability distributions of streamflow and floods by means of the PHysically-based Extreme Value (PHEV) distribution of river flows (Basso et al., 2021). This framework is grounded on a well-established mathematical description of precipitation, soil moisture, and runoff generation in river basins (Laio et al., 2001; Porporato et al., 2004; Botter et al., 2007b, 2009). Rainfall is described as a marked Poisson

https://doi.org/10.5194/egusphere-2023-660
Preprint. Discussion started: 2 May 2023

process with frequency $\lambda_p[\mathrm{T}^{-1}]$ and exponentially distributed depths with average α [L]. Soil moisture increases due to rainfall infiltration and decreases due to evapotranspiration. The latter is represented by a linear function of soil moisture between the wilting point and an upper critical value expressing the water holding capacity of the root zone. Runoff pulses occur with frequency $\lambda < \lambda_p$ when the soil moisture exceeds the critical value. These pulses replenish a single catchment storage, which drains according to a nonlinear storage-discharge relation. The related hydrograph recession is described via a power law function with exponent a $[-]$ and coefficient K $[\mathrm{L}^{1-a}/\mathrm{T}^{2-a}]$ (Brutsaert and Nieber, 1977), which allows for mimicking the joint effect of different flow components (Basso et al., 2015). Such a description of runoff generation and streamflow dynamics was successfully tested in a variety of hydro-climatic and physiographic conditions (Arai et al., 2020; Botter et al., 2007a; Botter et al., 2010; Ceola et al., 2010; Doulatyari et al., 2015; Mejía et al., 2014; Müller et al., 2014; Müller et al., 2021; Pumo et al., 2014; Santos et al., 2018; Schaefli et al., 2013).

PHEV provides a set of consistent expressions (Basso et al., 2021) for the probability distributions of daily streamflow, ordinary peak flows (i.e., local flow peaks occurring as a result of streamflow-producing rainfall events; *sensu* Miniussi et al., 2020), and floods (i.e., flow maxima in a certain timeframe; Basso et al., 2016). For example, the probability distribution of daily streamflow q can be expressed as (Botter et al., 2009):

$$p(q) = C_1 \cdot q^{-a} \left(e^{\frac{-1}{\alpha K(2-a)} \cdot q^{2-a}} \right) \left(e^{\frac{\lambda}{K(1-a)} \cdot q^{1-a}} \right), \tag{1}$$

where C_1 is a normalization constant.

Taking the limit of Eq. (1) for $q \to +\infty$ provides indications on the tail behavior of the flow distribution (Basso et al., 2015). This is determined by the three terms in the equation, namely, one power law and two exponential functions, which behave differently depending on the value of the hydrograph recession exponent a (Eq. 2; notice that $a > 1$ in most river basins; Biswal and Kumar, 2014; Tashie et al., 2020a).

$$\lim_{q \to +\infty} p(q) = \lim_{q \to +\infty} \left\{ C_1 \cdot \overbrace{q^{-a}}^{\mapsto 0} \left(\overbrace{e^{\frac{-1}{\alpha K(2-a)} \cdot q^{2-a}}}^{\mapsto 0 \;\; \mapsto e^0 = 1} \right) \left(\overbrace{e^{\frac{\lambda}{K(1-a)} \cdot q^{1-a}}}^{\mapsto e^0 = 1} \right) \right\}, \tag{2}$$

$\mapsto 0$ for $1 < a < 2$; $\mapsto e^0 = 1$ for $a > 2$

When $1 < a < 2$, the last term on the right-hand side converges to a constant value of one as q increases, thereby no more influencing how the distribution decreases toward zero. The first two terms instead decrease toward zero, affecting how the probability decreases for increasing values of q. The tail behavior is in this case determined by both a power law and an exponential function, indicating that the probability decreases faster than an exponential but slower than a power law. When $a > 2$, both the exponential terms converge to a constant value of one as q increases, and thus no more influence how the probability decreases toward zero. In this case the tail of the distribution is solely determined by the power law function.

https://doi.org/10.5194/egusphere-2023-660
Preprint. Discussion started: 2 May 2023

Despite being aware that several definitions of heavy-tailed distribution exist (El Adlouni et al., 2008; Vázquez et al., 2006), in the remainder of the manuscript we refer to distributions which exhibit a power law tail as heavy-tailed.

From the above derivations, the hydrograph recession exponent emerges as a key index of the tail behavior of streamflow distributions, which shall be heavy-tailed for values of $a > 2$. The same analysis applies to infer the tail behavior of the probability distributions of ordinary peak flows (Botter et al., 2009) and floods (Basso et al., 2016) (see Appx. A). Remarkably, we find that the same critical value of the recession exponent indicates the emergence of heavy-tailed behavior also in peak flow and flood distributions. Therefore, we propose the hydrograph recession exponent a as a physically-based index for identifying heavy-tailed flood behavior, test its capability to correctly predict such behavior in Sec. 4, and discuss the results in Sec. 5.

3 Data and parameter estimation

To test the proposed physically-based index of heavy-tailed flood behavior (i.e., the hydrograph recession exponent a), we use daily streamflow records of 98 gauges across Germany (Fig. C1). The analyzed river basins encompass a variety of climate and physiographic settings (Tarasova et al., 2020). Their areas range from 110 to 23,843 km^2 with a median value of 1,195 km^2. The length of the streamflow records range from 35 to 63 years with a median value of 58 years (inbetween 1951 – 2013).. We perform all analyses on a seasonal basis (winter: December–February, spring: March–May, summer: June–August, fall: September–November) to account for the seasonality of the hydrograph recessions (Tashie et al., 2020b) and flood distributions (Durrans et al., 2003). We term the analysis of a given river gauge during a season a case study. We select gauges for which processes driving streamflow dynamics are reasonably consistent with the adopted theoretical framework. Hence, we discard gauges affected by large dams, reservoirs (Lehner et al., 2011) and anthropogenic flow disturbances (based on visual examination; Tarasova et al., 2018). Case studies with strong snowfall (during a season), for which the average daily temperature is below zero degrees during precipitation events for over 50% of a season, are also discarded (i.e., only the affected season is removed from the analyses) . This results in an overall number of 386 case studies, including 97 case studies in spring, 96 in summer, 98 in autumn and 95 in the winter season.

We estimated the hydrograph recession exponent a for each case study as the median value of the exponents of power law functions fitted to $dq/dt - q$ pairs of individual hydrograph recession (Jachens et al., 2020; Biswal, 2021). Hydrograph recessions are composed of ordinary peak flows and the following streamflow values decreasing for a minimum duration of five days. The proposed index of heavy-tailed flood behavior can thus be estimated based on commonly available daily discharge observations.

To validate the identification of tail behavior obtained by means of the proposed index, we benchmark it against data by fitting a power law distribution to the empirical data distribution. A case study is considered to be heavy-tailed according to the observations if the fitted power law reliably describe the tail behavior of the data distribution. This is evaluated by means of a state-of-the-art method proposed by Clauset et al. (2009). The exponent b of the empirical power law is first computed by fitting a power law to the upper tail of the data distribution. An optimized lower boundary is determined by considering the

https://doi.org/10.5194/egusphere-2023-660
Preprint. Discussion started: 2 May 2023

best fit according to the Kolmogorov-Smirnov (KS) statistic, one of the most common measures of the distance between two non-normal distributions. The method then assesses whether the fitted power law reliably represents the observed data by using statistical tests, such as the Kolmogorov-Smirnov statistic and a Monte Carlo procedure, to verify that the residual errors between the data and the power law distribution fall within the range of fluctuations expected from random sampling. If the residual errors are found to be within the range of fluctuations expected from random sampling, the power law is deemed a reliable representation of the empirical data distribution (Appx. B). We use the python package plfit 1.0.3 to implement these computations and refer to Clauset et al. (2009) for further details concerning the approach.

We analyze three types of empirical data, namely daily streamflow, ordinary peaks, and monthly maxima , and obtain estimates of the fitted exponent *b* for each case. We use these results to validate the capabilities of the proposed index to infer heavy-tailed flood behavior from common hydrological dynamics, i.e., from the analysis of hydrograph recessions. We acknowledge that the benchmark we use, i.e., the empirical power law, may be influenced by fitting uncertainty due to data scarcity in some cases (i.e., especially when we analyse maxima; we indeed considered monthly maxima (Fischer and Schumann, 2016; Malamud and Turcotte, 2006) instead of the seasonal maxima previously used in the literature (e.g., Basso et al., 2021) to extend the sample size). The parallel analyses for cases with larger sample size (i.e., daily streamflow and ordinary peaks) provide more robust validation and support the interpretation of results for maxima. The topic is further discussed in Secs. 4 and 5.

4 Results

We examine if power law distributions fitted to the empirical distributions of daily streamflow, ordinary peaks, and monthly maxima well describe the observed data for case studies identified as having heavy-tailed behavior (i.e., $a > 2$) according to the process-based index. First, we identify the case studies with either heavy- ($a > 2$) or nonheavy ($a < 2$) -tailed behavior based on the process-based index. Then, we use the KS statistic κ to evaluate the reliability of the fitted power law distribution in describing the data ($\kappa \in [0,\infty]$, $\kappa=0$ denotes the highest reliability). Low values of the KS statistic κindicate that the empirical data are likely to be drawn from a power law. Figs. 1a-1c show that the histograms of the number of case studies for decreasing values of the KS statistic are significantly skewed (i.e., the skewness is significantly different from zero) toward lower values of κ for all cases of daily streamflows, ordinary peak flows, and monthly flow maxima with $a > 2$ (red histograms), whereas this is not true for cases with $a < 2$ (green histograms) (i.e., the skewness is not significantly different from zero in these cases). Statistical significance of the skewness was evaluated through the Jarque–Bera test at a significance level of 0.05. The result indicates that data from case studies which are identified with heavy-tailed behavior according to the process-based index ($a>2$, red) are indeed more likely to come from power law distributions.

We further estimate the accuracy of the process-based index based on the fraction of case studies that are identified as heavy-tailed by the proposed index among all cases that are heavy-tailed according to the available observations. To define the latter, we set a threshold value of κ: the power law is a reliable representation of the data for cases with κ below the threshold.

https://doi.org/10.5194/egusphere-2023-660
Preprint. Discussion started: 2 May 2023

Mathematically, the accuracy can be expressed as $P(a > 2|\kappa < \kappa_r) = N_c(a > 2|\kappa < \kappa_r)/N_c(\kappa < \kappa_r)$, where κ_r is the imposed threshold of κ, $N_c(\kappa < \kappa_r)$ is the number of case studies whose $\kappa < \kappa_r$, and $N_c(a > 2|\kappa < \kappa_r)$ is the number of case studies with $a > 2$ among the $N_c(\kappa < \kappa_r)$ case studies. Higher accuracy essentially means that a higher fraction of heavy-tailed cases is correctly identified by means of the process-based index. Notice that the smaller the κ_r threshold, the more reliable is the description of the data through power law distributions.

Figs. 1d-1f display the accuracy of the process-based index as a function of the reliability threshold κ_r. In all three cases (daily streamflows, ordinary peak flows, and monthly flow maxima), the accuracy values increase with the reliability level of the power law distribution fitted on observed data. This means that the process-based index shows high accuracy for case studies where the empirical distributions of observed data are more consistent with power laws. In other words the proposed index, which is estimated from common streamflow dynamics as the hydrograph recession exponent, accurately identifies heavy-tailed behavior of streamflow and flood distributions displayed by the available observations.

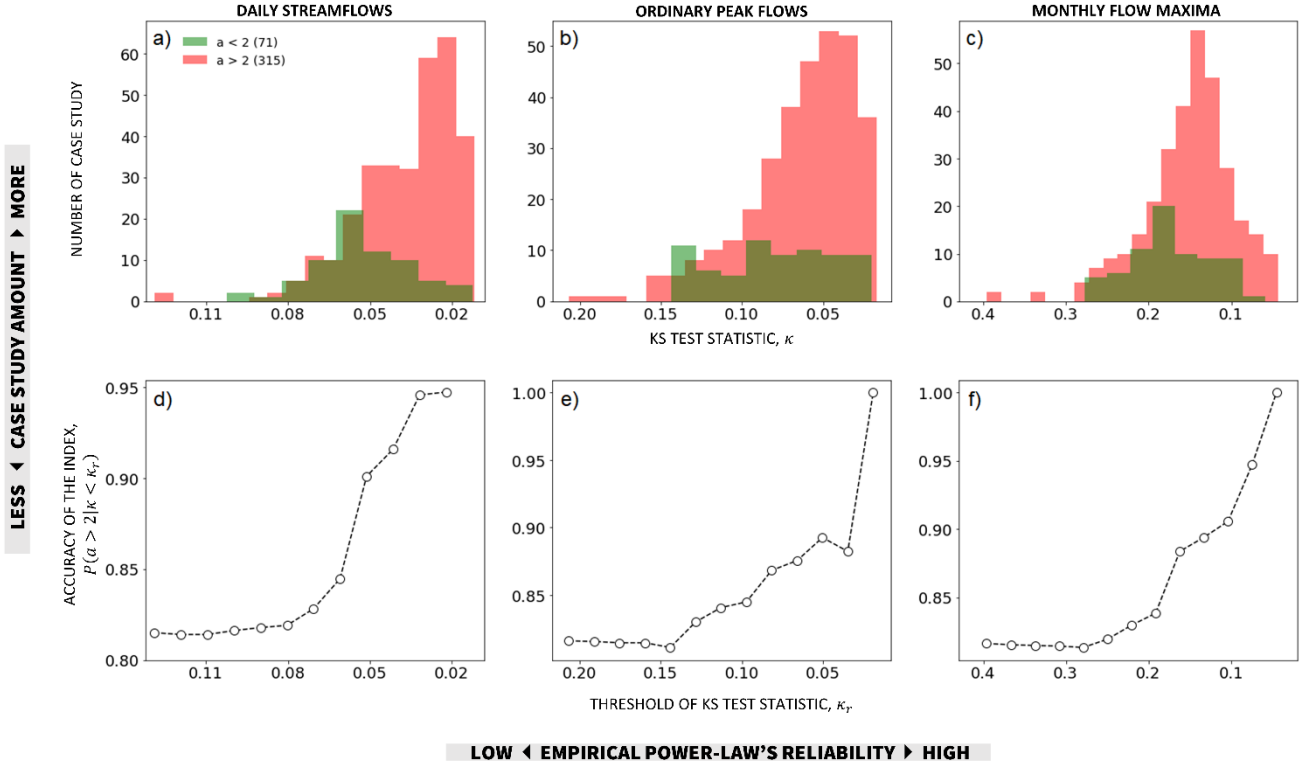

Figure 1. Accuracy of the proposed process-based index. (a)-(c) Number of analyzed case studies as a function of the KS statistic κ of empirically fitted power law distributions (the latter is a measure of how reliable the power law is as a model for the given data: the lower κ, the more reliable the power law model). Case studies are identified as having either heavy- ($a > 2$, red histograms) or nonheavy ($a < 2$, green histograms) –tailed behavior based on the hydrograph recession exponent a estimated from daily flow records, which is proposed as a process-based index of heavy-tailed streamflow and flood behavior. (d)-(f) Accuracy of the process-based index as a function of

https://doi.org/10.5194/egusphere-2023-660
Preprint. Discussion started: 2 May 2023

decreasing thresholds of κ_r (i.e., increasing reliability of empirical power laws). The values of the KS statistic κ are derived from records of (a, d) daily streamflows, (b, e) ordinary peak flows, and (c, f) monthly flow maxima.

We further employ the goodness-of-fit testing procedure proposed by Clauset et al. (2009) (Appx. B) to identify case studies for which the representation of daily streamflow, ordinary peak flows, and monthly maxima by means of power law distributions is convincingly supported by the available data. We refer to these case studies as 'confirmed heavy-tailed cases' (Fig. 2, black dots). Conversely, we term the remaining ones as 'uncertain cases' (Fig. 2, gray). The latter label denotes the fact that it cannot be determined with certainty whether the distributions underlying the available observations in these cases are or not power laws due to scarcity of data.

Fig. 2 shows the empirical power law exponent b as a function of the process-based index of heavy-tailed behavior a. Red markers display the median values of a and b (squares), the interquartile intervals of b (vertical bars), and the binning ranges of a (horizontal bars, equal number of case studies in each bin), highlighting the correlation between the empirical power law exponent b and the hydrograph recession exponent a for confirmed heavy-tailed cases (black dots) in all three cases (i.e., daily streamflows, ordinary peak flows, and monthly flow maxima). We test the correlation by calculating their distance (Székely et al., 2007) and Spearman (Spearman, 1904) correlations, which are valid for both linear and nonlinear associations between random variables. We find that a and b are significantly correlated at a significance level of 0.05 in all three cases with distance (Spearman) correlation coefficients of 0.45, 0.44, and 0.81 (0.42, 0.46, and 0.60) for daily streamflows, ordinary peak flows, and monthly flow maxima. The high values of the correlation coefficients for monthly flow maxima are likely affected by the existence of two clusters in Fig. 2c. Nonetheless, the existence of a statistically significant correlation between the empirical power law exponent and the process-based index, obtained for panels a, b, and c, confirms that the process-based index not only can be used to identify heavy-tailed flood behavior (as Fig. 1 shows) but also to evaluate the degree of the tail heaviness of the underlying distributions.

Fig. 2c is of particular interest because it shows an example of the typical limitations of methods that rely solely on observations to determine the tail behavior of the distribution of maxima (e.g., Papalexiou and Koutsoyiannis, 2013) and, at the same time, highlights the power of the proposed process-based index. Large values of the recession exponent a, in agreement with corresponding large values of b, are found for all confirmed heavy-tailed cases (black dots in Fig. 2c) where the power law provides a plausible representation of the empirical distribution of monthly maxima. For uncertain cases (gray dots in Fig. 2c) the values of the empirical power law exponents are unreliable (according to the applied method; Clauset et al., 2009) since it cannot be determined with certainty whether the empirical distributions are or not power laws due to data scarcity. Conversely, the hydrograph recession exponent is calculated from daily streamflow data. We can therefore identify cases with heavy-tailed behavior and evaluate their tail heaviness based on the values of a. This estimate is deemed robust, provided that the predictions

https://doi.org/10.5194/egusphere-2023-660
Preprint. Discussion started: 2 May 2023

of the proposed index are confirmed by observations in cases (panels a and b) where data size is not a limitation (i.e., for daily streamflow and ordinary peak flows).

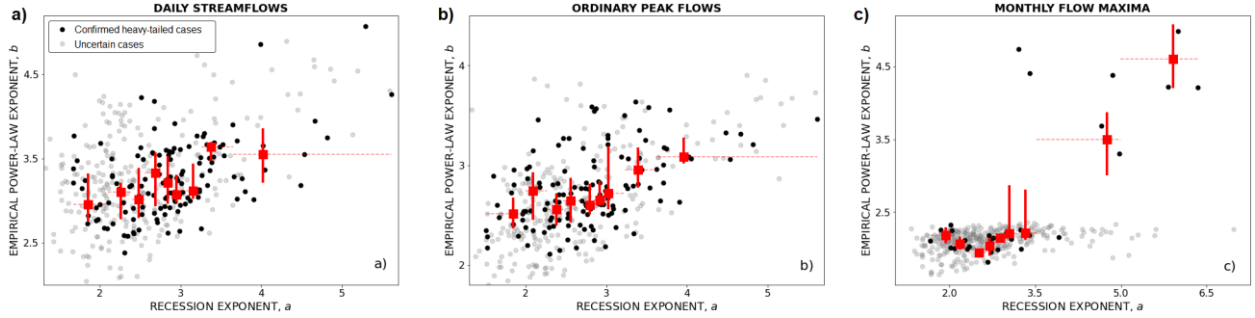

Figure 2. Empirical power law exponent b as a function of the process-based index of heavy-tailed behavior a. Case studies are classified into groups of confirmed heavy-tailed (black dots) and uncertain (gray dots) cases on the basis of the hypothesis test (Appx. B; Clauset et al., 2009). The former denotes cases for which a power law provides a reliable description of the empirical data distribution, while the latter denotes cases whose data cannot convincingly support such a distribution. Red markers highlight the correlation between the empirical power law exponent b and the hydrograph recession exponent a for confirmed heavy-tailed cases in the case of (a) daily streamflows (n=121 case studies), (b) ordinary peak flows (n=116), and (c) monthly flow maxima (n=34). Red markers display the median values of a and b (squares), the interquartile intervals of b (vertical bars), and the binning ranges of a (horizontal bars, equal number of case studies in each bin).

In Fig. 3 we test the stability of the categorization of case studies into heavy/nonheavy-tailed flood behavior provided by the process-based index (i.e., the hydrograph recession exponent a) for decreasing data lengths. We compare results for the process-based index against two other frequently used metrics of heavy tails in hydrological studies: (1) the upper tail ratio (UTR) (Lu et al., 2017; Smith et al., 2018; Villarini et al., 2011) and (2) the shape parameter ξ of the GEV distribution (Morrison and Smith, 2002; Papalexiou et al., 2013; Villarini and Smith, 2010). The UTR is defined as the ratio of the flood of record to the 0.9 quantile of floods (Smith et al., 2018) here represented by monthly flow maxima, while ξ is estimated by fitting a GEV distribution on the sample of monthly maxima using the python package OpenTURNS 1.16 (Baudin et al., 2017). For all three indices ($a, UTR,$ and ξ), we estimate their values for data lengths decreasing from 35 (i.e., the shortest entire record length in the dataset) to 2 years. We acknowledge that estimating parameters of extreme value distributions from such short records is not recommended. However, the exercise highlights the perks of a process-based index that, as it will be shown, is able to provide robust results also when short data series only are available. For each case study, we obtain 30 samples with the assigned test length from the entire data series using resampling without substitution. For each test length, we calculate the median values of the indices estimated from these samples, and plot them in Fig. 3 together with their variability across case studies (vertical shaded bars and lines in Fig. 3 show the 0.25–0.75 and 0.05–0.95 quantile ranges of the index estimates across case studies).

To evaluate the consistency of the categorization of tail behavior across different data lengths we proceed as follows. For each case we first compute the hydrograph recession exponent and GEV shape parameter from the entire data record and denote them with an asterisk superscript (i.e., a^* or ξ^*). Heavy-tailed cases are defined as having $a^*>2$ or $\xi^*>0$ (Godrèche et al., 2015), while non-heavy-tailed cases have values below these thresholds. To visualize heavy-tailed and non-heavy-tailed behaviors,

https://doi.org/10.5194/egusphere-2023-660
Preprint. Discussion started: 2 May 2023

we mark them in Fig. 3 in red and green colors, respectively, based on the reference values obtained from the entire data record. We then recalculate the indices from shorter samples and evaluate whether their values are consistent with the above categorization. For the UTR, we cannot implement this approach because there is no specific threshold for the identification of heavy/nonheavy tails. We therefore directly compare the stability of the UTR's values across data lengths (a larger value indicates a heavier tail).

The physically-based index provides consistent categorization of heavy/nonheavy-tailed flood behavior across varying data lengths (Fig. 3a). The index estimates remain above 2 for most heavy-tailed cases (red) and below 2 for most nonheavy-tailed cases (green) (as defined according to the reference value a^* computed using the entire data record) when the data length decreases. The index estimates demonstrate the consistency throughout the test data length, as evidenced by the narrow range of variation in the median values of the estimates. For heavy-tailed cases, the median values ranged from 2.64 to 2.92, while for nonheavy-tailed cases, they ranged from 1.84 to 2.0. Additionally, the coefficient of variation for the estimates remained relatively constant, ranging from 0.29 to 0.33 for both heavy and nonheavy-tailed cases. This indicates that the variability of the results (vertical shaded bars and lines in Fig. 3) is mostly due to pooling together different case studies belonging to the same category (heavy or nonheavy-tailed), and does not increase as a result of decreasing length of the available data.

In contrast, the upper tail ratio shows pronounced instability for decreasing data lengths (Fig. 3b). The median value of the index estimates varies between 1.32 and 2.36, with a coefficient of variation ranging from 0.15 to 0.64. These values indicate uncertain assessments based on the UTR and its tendency to underestimate the tail heaviness as the data length decreases.

Fig. 3c depicts the categorization of tail behavior using GEV shape parameter estimates. The results show that to achieve stable and consistent categorization of heavy-tailed behavior, a minimum test data length of 5 years is recommended. Underestimation of heavy-tailed behavior occurs with shorter data lengths. Although the median values of ξ range from 0.39 to 0.52 for the heavy-tailed cases and is equal to 0 for the nonheavy-tailed cases, the coefficient of variation shows some

https://doi.org/10.5194/egusphere-2023-660
Preprint. Discussion started: 2 May 2023

255 variation across the test data length, ranging from 0.37 to 1.03 for heavy-tailed cases. The coefficient of variation is not applicable for nonheavy-tailed cases due to their zero mean values.

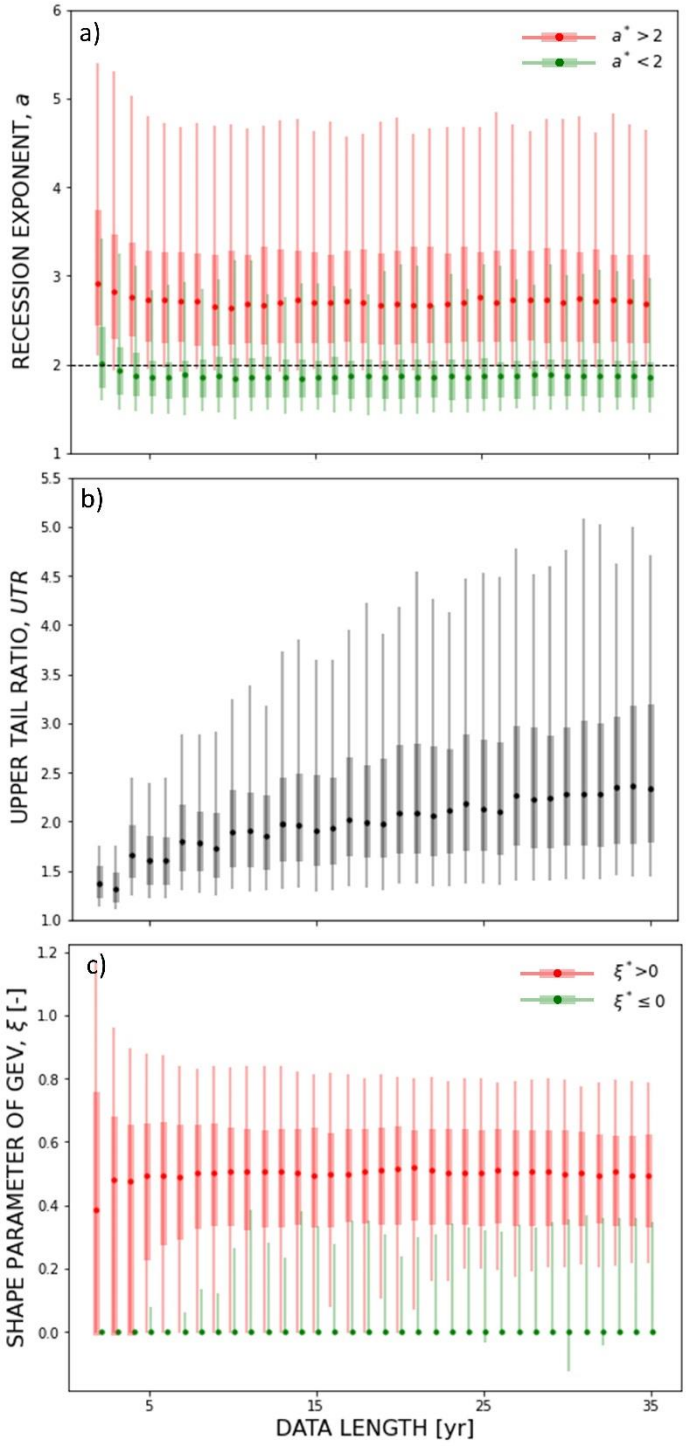

https://doi.org/10.5194/egusphere-2023-660
Preprint. Discussion started: 2 May 2023

Figure 3. Stability of the categorization of case studies into heavy/nonheavy-tailed flood behavior for decreasing data lengths. Estimates of three different indices of tail behavior as a function of data length. (a) Hydrograph recession exponent a (i.e., the proposed process-based index of this study). Two frequently used metrics of heavy tails in hydrological studies: (b) the upper tail ratio UTR, and (c) the shape parameter ξ of the GEV distribution. Dots display the median values of the estimates for 386 case studies; vertical shaded bars and lines show the 0.25-0.75 and 0.05-0.95 quantile ranges of the estimates, respectively. The entire data record was used for computing the reference values of the hydrograph recession exponent a^* and the GEV shape parameter ξ^* and categorizing each case study as either having (red) or not (green) the heavy-tailed behavior.

5 Discussion

Assessment of flood tail behavior is challenging due to high levels of uncertainty arising from the scarcity of data on floods, which are by definition rare events. This issue is particularly prominent when maxima are used in the analysis as in the annual maximum approach. Despite the widespread use of this method, its limitations for what concerns the reliability of flood tail estimates are well recognized. Very large sample sizes are indeed essential for obtaining accurate prediction of tail behavior (Papalexiou and Koutsoyiannis, 2013).

To address the challenge of obtaining reliable estimates, alternative methods have been proposed. A frequently used approach is the peak-over-threshold analysis, which uses the information content of a larger sample of data (Lang et al., 1999; Pan et al., 2022). Previous studies have demonstrated that this method leads to lower uncertainty in estimating high floods (Kumar et al., 2020). Volpi et al. (2019) also showed the advantage of using all the available observations (i.e., not only the peaks over a certain threshold) for estimating extreme events. In summary, all these methods suggest that discharge values other than maxima can provide information about the characteristics of extreme events. Specifically, incorporating information from less extreme (but more numerous) observations can reduce the uncertainty in the estimation of extreme events and lead to improved accuracy. Furthermore, non-asymptotic methods suggest that extremes are realizations of the underlying ordinary events (Marani and Ignaccolo, 2015; Lombardo et al., 2019), which can thus be used to assess rare events. These methods have significantly improved the estimation of extreme values with lower uncertainty (Marra et al., 2018; Miniussi and Marani, 2020; Mushtaq et al., 2022; Hu et al., 2023).

Similarly to the latter approaches, the index introduced in this study (i.e., the hydrograph recession exponent) leverages information on ordinary discharge dynamics to infer the tail behavior of flood distributions. This approach entails some advantages: firstly, it effectively extracts information from a larger amount of available streamflow data. Secondly, estimating the hydrograph recession exponent requires significantly less data than conventional approaches that involve fitting probability distributions to hydrological samples, while providing reliable results. But most importantly, the proposed index offers a mechanistic approach to understand the emergence of heavy-tailed flood behavior, thus providing a process-based alternative to methods that solely rely on statistical analysis of observations. The importance of understanding intrinsic watershed dynamics which promote the occurrence of extreme events and contributing factors that lead to heavy-tailed flood behavior (Tarasova et al., 2020) was recently highlighted in a comprehensive review by Merz et al. (2022). Identify reliable proxies for inferring such behavior (*sensu* Wilson and Toumi, 2005) is as well important. The proposed index, which represents such a

https://doi.org/10.5194/egusphere-2023-660
Preprint. Discussion started: 2 May 2023

proxy grounded on intrinsic hydrologic dynamics of the river basin, is thus especially useful in the very common cases when the tail of the flood distribution cannot be known from limited available observations.

The hydrograph recession exponent (which is the identified index of heavy-tailed flood behavior) essentially represents the nonlinearity of the storage-discharge response in catchments (Wittenberg, 1999; Biswal and Marani, 2010). A higher degree of nonlinearity leads to higher peak flows and heavier tail of the streamflow distribution (Basso et al., 2015). In agreement with these findings, former simulation-based and field studies have shown that high nonlinearity of the catchment hydrological response linked to an increase of the runoff contributing area results in a marked increase of the slope of flood frequency curves (Fiorentino et al., 2007; Rogger et al., 2012), which may be indicative of a heavy-tailed flood behavior. Gioia et al. (2012) also demonstrated that a nonlinear catchment response can convert light-tailed rainfall inputs into flood distributions with heavy tails, further confirming the role of nonlinear storage-discharge responses in producing heavy-tailed flood behavior. Based on a mechanistic description of hydrological dynamics and validation with observations from a large dataset, our findings directly demonstrate that heavy-tailed flood behaviors emerge as a result of the nonlinearity of the catchment hydrologic response, which can thus be used as a metric to assess tail behaviour of flood distributions from common streamflow dynamics.

The findings in Fig. 2 showcase the drawbacks of relying on purely statistical data analyses (which supply the empirical power law exponents b) to identify flood tail behaviors and the advantages of adopting the mechanistic approach proposed in this study (which yield the hydrograph recession exponent a). The gray markers in Fig. 2 indicate uncertainty in determining whether the distribution has a power law tail, which is shown to be more prevalent when the sample size is reduced, based on statistical analyses according to the Clauset (2009) method (69%, 70%, and 91% of the case studies for daily streamflow, ordinary peaks, and monthly maxima, respectively). The physically-based index proposed in this study offers a solution to these limitations. Our proposed index is shown to perform well in cases where statistical methods may be limited due to a lack of data, as confirmed by the significant correlations between the recession exponent and the reliably empirical power law exponent in all three panels (represented by black dots in Fig. 2). Even in cases where the statistical method is unable to confirm the underlying distribution (e.g., monthly maxima in panel c), our proposed index can still provide robust estimates of tail heaviness based on the values of recession exponents. This is supported by the analyses of daily streamflows and ordinary peaks, where sample size is not a limitation and the predictions of the proposed index are confirmed by observations. Overall, our physically-based index offers a promising solution for accurately characterizing the tail behavior of flood distributions, especially when traditional statistical methods may be limited due to a lack of data.

Data scarcity is a major challenge for reliable flood hazard assessment, mainly because of relatively short hydrological data records worldwide (Lins, 2008). The availability of a robust index of heavy-tailed flood behavior that work even with short data records is desirable. We test three indices, namely the recession exponent (the proposed index), the upper tail ratio (UTR), and the shape parameter of the Generalized Extreme Value (GEV) distribution (ξ), for categorizing tail behavior for decreasing data lengths. The results (Fig. 3a) show that the recession exponent provides stable estimates and categorizes cases consistently into heavy or non-heavy tails for decreasing data lengths. Furthermore, the slight variation in the estimates of the recession

https://doi.org/10.5194/egusphere-2023-660
Preprint. Discussion started: 2 May 2023

exponent for each test data length implies that variation in estimates primarily arises from case study heterogeneity rather than decreasing data length. Conversely, UTR significantly underestimates both the tail heaviness and the variation across cases for decreasing data lengths (Fig. 3b). In agreement with previous studies, underestimation of tail heaviness occurred using UTR when the sample size was small (Smith et al., 2018; Wietzke et al., 2020). Meanwhile, the categorization of tail behavior was stable for cases with dataset longer than 5 years using the GEV shape parameter. However, high uncertainty in the variation of estimates across cases is observed when available data is relatively short as also highlighted by previous studies (e.g., Wietzke et al., 2020) (Fig. 3c). Implied by this observation is that the estimates are biased by the short analyzed data and a longer data record is desirable for a more reliable fitting of a GEV on data (Papalexiou and Koutsoyiannis, 2013).

The hydrograph recession exponent allows at least two significant applications as a proxy for heavy-tailed flood behavior. Firstly, it can be directly used to improve comparability across catchments and provide a fair assessment of mapping regional patterns of flood hazards (Merz et al., 2022). Traditionally, assessing flood behavior across catchments using the same record length has been preferred (Cunderlik and Burn, 2002), but this is often not possible due to differences in data availability. The proposed index can robustly estimate heavy-tailed flood behavior from data with different record lengths, overcoming this limitation. Secondly, it can be applied as a preliminary step to correctly identify whether a considered catchment exhibits heavy-tailed flood behavior or not, and to select an appropriate probability distribution to be used in flood frequency analysis. This prior identification of tail behavior is crucial to avoid potential underestimation of flood extremes. (Miniussi et al., 2020; Mushtaq et al., 2022).

6 Conclusions

A new index of heavy-tailed flood behavior is identified from a physically-based description of streamflow dynamics. The new index is embodied by the hydrograph recession exponent and can be readily estimated from daily streamflow records. Our findings demonstrate that this index enables the identification of heavy or nonheavy tailed flood behaviors in a large set of case studies across Germany. Importantly, it provides an evaluation of the tail heaviness (i.e., the severity of flood risks) based on analyses of common discharge dynamics, and remarkably, the results remain robust even with limited data records.

The proposed index addresses the main limitations of current approaches, including the lack of physical support and low reliability in cases with limited data records. By extracting more information from available data and manifesting the nonlinearity of catchment response, it represents a reliable method to select suitable underlying distributions for flood frequency analyses and assess the peril of extreme floods in data poor areas.

Acknowledgments

This work is funded by the Deutsche Forschungsgemeinschaft-Project 421396820 “Propensity of rivers to extreme floods: climate-landscape controls and early detection (PREDICTED)” and FOR 2416 “Space-Time Dynamics of Extreme Floods

https://doi.org/10.5194/egusphere-2023-660
Preprint. Discussion started: 2 May 2023

(SPATE)". The financial support of the Helmholtz Centre for Environmental Research and the Norwegian Institute for Water Research is as well acknowledged. SY (the 3rd author) acknowledges the support of the Helmholtz Climate Initiative Project funded by the Helmholtz Association. The manuscript and supporting information provide all the information needed to replicate the results.

Data Availability Statement

For providing the discharge data for Germany, we are grateful to the Bavarian State Office of Environment (LfU, https://www.gkd.bayern.de/de/fluesse/abfluss) and the Global Runoff Data Centre (GRDC) prepared by the Federal Institute for Hydrology (BfG, http://www.bafg.de/GRDC). Climatic data can be obtained from the German Weather Service (DWD; ftp://ftp-cdc.dwd.de/pub/CDC/). The digital elevation model can be retrieved from Shuttle Radar Topography Mission (SRTM; https://cgiarcsi.community/data/srtm-90m-digital-elevation-database-v4-1/).

Appendix A Identifying tail behavior for distributions of peak flows and flow maxima from hydrological processes

The probability distribution of ordinary peak flows and flow maxima can be analytically expressed as $p_j(q)$ and $p_M(q)$, respectively (Basso et al., 2016):

$$p_j(q) = C_2 \cdot q^{1-a} \cdot e^{-\frac{q^{2-a}}{aK(2-a)}} \cdot e^{\frac{q^{1-a}}{K(1-a)}}, \quad \text{(A1)}$$

$$p_M(q) = p_j(q) \cdot \lambda\tau \cdot e^{-\lambda\tau \cdot D_j(q)}, \quad \text{(A2)}$$

$$D_j(q) = \int_q^{\infty} p_j(q)\, dq, \quad \text{(A3)}$$

where $\tau[day]$ is the duration of the specified time frame, C_2 is normalization constants, and all the other notations have been listed in the main context.

To analyze the tail behavior of these distributions, we take the limit of $q \longrightarrow +\infty$ for both Eq. A1 and A2. Because $\lim_{q\to\infty} D_j(q) = \int_{\infty}^{\infty} p_j(q)\, dq = 0$, the Eq. A1 and A2 can be transformed into: (set $C_3 = \lambda\tau C_2$)

https://doi.org/10.5194/egusphere-2023-660
Preprint. Discussion started: 2 May 2023

$$\lim_{q\to+\infty} p_j(q) = \lim_{q\to+\infty}\left\{C_2 \cdot \overbrace{q^{1-a}}^{\mapsto 0}\left(\overbrace{e^{\frac{-1}{\alpha K(2-a)}\cdot q^{2-a}}}^{\mapsto 0}\right)\right\}, \quad \begin{matrix}\text{for } 1<a<2 \\ \\ \text{for } a>2\end{matrix} \tag{A4}$$
$$\mapsto e^0 = 1$$

$$\lim_{q\to+\infty} p_M(q) = \lim_{q\to+\infty}\left\{C_3 \cdot \overbrace{q^{1-a}}^{\mapsto 0}\left(\overbrace{e^{\frac{-1}{\alpha K(2-a)}\cdot q^{2-a}}}^{\mapsto 0}\right)\right\}, \quad \begin{matrix}\text{for } 1<a<2 \\ \\ \text{for } a>2\end{matrix} \tag{A5}$$
$$\mapsto e^0 = 1$$

For both of the cases, the tail behavior is determined by a power law term and an exponential term when $1 < a < 2$, which indicates the tail decreases slower than the exponential but faster than the power law tail; while the tail behavior is solely determined by a power law function, representing heavy-tailed flow distribution when $a > 2$. Therefore, the hydrograph recession exponent ($a > 2$) is shown as an indicator of the heavy-tailed flood behavior.

Appendix B Goodness-of-fit tests for the empirical power laws

To test if the empirical power law is a plausible underlying distribution of the observed data, we follow the hypothesis test proposed by Clauset et al. (2009). The null hypothesis is 'The empirical power law is a plausibly underlying distribution of the observed data.' Residual errors exist between the empirical power law and the observed data, which can be estimated by the error distance ε_d by means of the Kolmogorov-Smirnov statistic. The Kolmogorov-Smirnov test is selected because it is one of the most common measures for non-normal data. The core of the hypothesis test is to statistically prove that the errors between the data and the power law (i.e., ε_d) are rational fluctuation of sampling randomness rather than being drawn from an incorrect underlying distribution. To determine the rationality of the sampling randomness, a Monte Carlo procedure is introduced: (1) a large number of groups n of synthetic data (with the same size as the observed data) are randomly generated from the empirical power law; (2) the error distance ε_{s_i} of each synthetic group to the empirical power law is calculated for $i = 1,2,\cdots,n$; (3) the frequency of $\varepsilon_s > \varepsilon_d$ defines the p-value of the hypothesis test, which indicates the probability that the residual errors between the empirical power law and the observed data locates within the range of sampling randomness fluctuations; and (4) the rationality is determined by $p > 0.1$ using this package.

When $p \leq 0.1$, the null hypothesis is rejected; that is, the observed data are not plausibly drawn from the empirical power law. On the contrary, the empirical power law is considered a plausible distribution for the observed data for their residual errors

https://doi.org/10.5194/egusphere-2023-660
Preprint. Discussion started: 2 May 2023

are statistically rational fluctuation of sampling randomness when $p > 0.1$. Notice that a greater p-value is better in this case because the aim is to verify the null hypothesis rather than to indicate it is unlikely to be correct, as others often considered. Thus $p > 0.1$ is a more rigorous setting than $p > 0.05$ in this case.

The setting of $n = 1000$ is used as an adequate (great enough) number of iterations in this framework to distinguish underlying distributions that are commonly mixed (as suggested by Clauset et al. (2009)).

The hypothesis test of the empirical power law including all the above procedures can be implemented via the function test_pl in the python package plfit 1.0.3 (https://pypi.org/project/plfit/).

It is worth mentioning that, statistically, we cannot say those who do not pass the hypothesis test 'are not' power law distributions. There are at least two potential reasons for this result: (1) they are indeed not power law functions, or (2) the underlying distribution cannot be concluded due to the high uncertainty in the empirical data with small sample sizes. We thus use the term 'uncertain cases' to indicate this awareness in the main manuscript.

https://doi.org/10.5194/egusphere-2023-660
Preprint. Discussion started: 2 May 2023

Appendix C A reference map of gauges across Germany used in this study

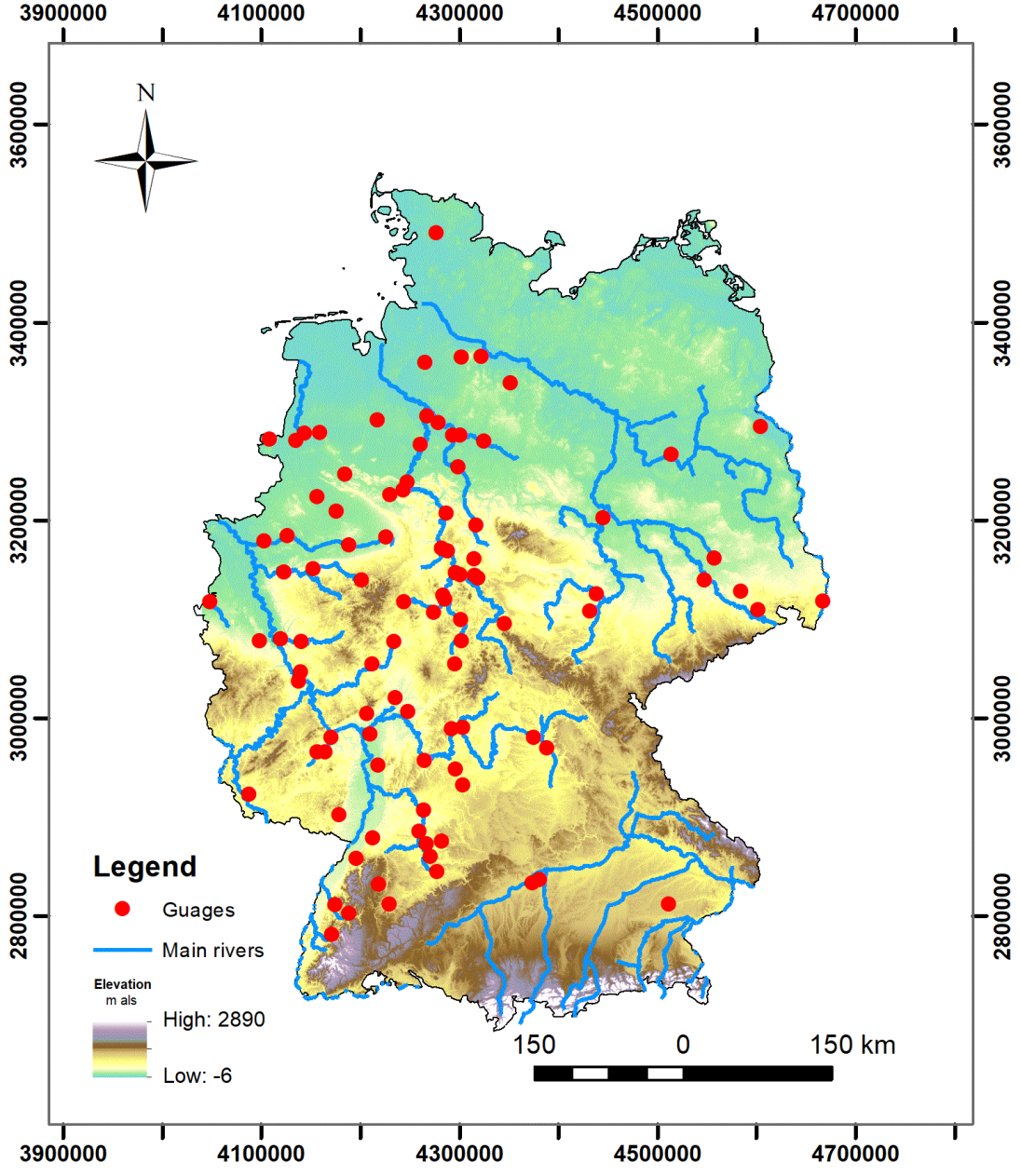

Figure C1 A reference map of gauges across Germany used in this study. These river basins encompass a variety of climate and physiographic settings without strong impact from dams and snowfall. Their areas range from 110 to 23,843 km^2 with a median value of 1,195 km^2. The minimum, median, and maximum lengths of the daily streamflow records are 35, 58, and 63 years (inbetween 1951 – 2013).

https://doi.org/10.5194/egusphere-2023-660
Preprint. Discussion started: 2 May 2023

Author contributions

H.-J. Wang: Conceptualization (lead); methodology (lead); investigation (lead); formal analysis (lead); writing – original draft (lead); writing – review and editing (equal).

R. Merz: Conceptualization (supporting); methodology (supervision); investigation (supervision); formal analysis (supervision); writing – review and editing (equal).

S. Yang: Investigation (supporting); formal analysis (supervision); writing – review and editing (equal).

S. Basso: Conceptualization (supporting); methodology (supervision); investigation (supervision); formal analysis (supervision); writing – review and editing (equal).

Declaration of interests

The authors declare that they have no known competing financial interests or personal relationships that could have appeared to influence the work reported in this paper.

References

Arai, R., Toyoda, Y., and Kazama, S.: Runoff recession features in an analytical probabilistic streamflow model, J. Hydrol., 597, 125745, https://doi.org/10.1016/j.jhydrol.2020.125745, 2020.

Basso, S., Botter, G., Merz, R., and Miniussi, A.: PHEV! The PHysically-based Extreme Value distribution of river flows, Environ. Res. Lett., 16, https://doi.org/10.1088/1748-9326/ac3d59, 2021.

Basso, S., Schirmer, M., and Botter, G.: On the emergence of heavy-tailed streamflow distributions, Adv. Water Resour., 82, 98–105, https://doi.org/10.1016/j.advwatres.2015.04.013, 2015.

Basso, S., Schirmer, M., and Botter, G.: A physically based analytical model of flood frequency curves, Geophys. Res. Lett., 43, 9070–9076, https://doi.org/10.1002/2016GL069915, 2016.

Baudin, M., Dutfoy, A., Iooss, B., and Popelin, A.-L.: OpenTURNS: An Industrial Software for Uncertainty Quantification in Simulation BT - Handbook of Uncertainty Quantification, edited by: Ghanem, R., Higdon, D., and Owhadi, H., Springer International Publishing, Cham, 2001–2038, https://doi.org/10.1007/978-3-319-12385-1_64, 2017.

Beirlant, J., Goegebeur, Y., Teugels, J., Segers, J., De Waal, D., and Ferro, C.: Statistics of extremes: Theory and applications, https://doi.org/https://doi.org/10.1002/0470012382, 2004.

Bevere, L. and Remondi, F.: Natural catastrophes in 2021: the floodgates are open, Swiss Re Institute sigma research, 2022.

https://doi.org/10.5194/egusphere-2023-660
Preprint. Discussion started: 2 May 2023

Biswal, B.: Decorrelation is not dissociation: There is no means to entirely decouple the Brutsaert-Nieber parameters in streamflow recession analysis, Adv. Water Resour., 147, 103822, https://doi.org/https://doi.org/10.1016/j.advwatres.2020.103822, 2021.

Biswal, B. and Kumar, D. N.: Study of dynamic behaviour of recession curves, Hydrol. Process., 792, 784–792, https://doi.org/10.1002/hyp.9604, 2014.

Biswal, B. and Marani, M.: Geomorphological origin of recession curves, Geophys. Res. Lett., 37, 1–5, https://doi.org/10.1029/2010GL045415, 2010.

Botter, G., Basso, S., Porporato, A., Rodriguez-Iturbe, I., and Rinaldo, A.: Natural streamflow regime alterations: Damming of the Piave river basin (Italy), Water Resour. Res., 46, 1–14, https://doi.org/10.1029/2009WR008523, 2010.

Botter, G., Peratoner, F., Porporato, A., Rodriguez-Iturbe, I., and Rinaldo, A.: Signatures of large-scale soil moisture dynamics on streamflow statistics across U.S. climate regimes, Water Resour. Res., 43, 1–10, https://doi.org/10.1029/2007WR006162, 2007a.

Botter, G., Porporato, A., Rodriguez-Iturbe, I., and Rinaldo, A.: Basin-scale soil moisture dynamics and the probabilistic characterization of carrier hydrologic flows: Slow, leaching-prone components of the hydrologic response, Water Resour. Res., 43, 1–14, https://doi.org/10.1029/2006WR005043, 2007b.

Botter, G., Porporato, A., Rodriguez-Iturbe, I., and Rinaldo, A.: Nonlinear storage-discharge relations and catchment streamflow regimes, Water Resour. Res., 45, 1–16, https://doi.org/10.1029/2008WR007658, 2009.

Brutsaert, W. and Nieber, J. L.: Regionalized drought flow hydrographs from a mature glaciated plateau, Water Resour. Res., 13, 637–643, https://doi.org/10.1029/WR013i003p00637, 1977.

Ceola, S., Botter, G., Bertuzzo, E., Porporato, A., Rodriguez-Iturbe, I., and Rinaldo, A.: Comparative study of ecohydrological streamflow probability distributions, Water Resour. Res., 46, 1–12, https://doi.org/10.1029/2010WR009102, 2010.

Clauset, A., Shalizi, C. R., and Newman, M. E. J.: Power-law distributions in empirical data, SIAM Rev., 51, 661–703, https://doi.org/10.1137/070710111, 2009.

Cooke, R. M., Nieboer, D., and Misiewicz, J.: Fat-Tailed Distributions: Data, Diagnostics and Dependence, volume 1., John Wiley & Sons, 2014.

Cooke, R. M. and Nieboer, D.: Heavy-Tailed Distributions: Data, Diagnostics, and New Developments, Resour. Futur. Discuss. Pap., No. 11-19, https://doi.org/dx.doi.org/10.2139/ssrn.1811043, 2011.

Cunderlik, J. M. and Burn, D. H.: The use of flood regime information in regional flood frequency analysis, Hydrol. Sci. J., 47, 77–92, https://doi.org/10.1080/02626660209492909, 2002.

Doulatyari, B., Betterle, A., Basso, S., Biswal, B., Schirmer, M., and Botter, G.: Predicting streamflow distributions and flow duration curves from landscape and climate, Adv. Water Resour., 83, 285–298, https://doi.org/10.1016/j.advwatres.2015.06.013, 2015.

Durrans, S. R., Eiffe, M. A., Thomas, W. O., and Goranflo, H. M.: Joint Seasonal /Annual Flood Frequency Analysis, J. Hydrol. Eng., 8, 181–189, https://doi.org/10.1061/(asce)1084-0699(2003)8:4(181), 2003.

El Adlouni, S., Bobée, B., and Ouarda, T. B. M. J.: On the tails of extreme event distributions in hydrology, J. Hydrol., 355, 16–33, https://doi.org/10.1016/j.jhydrol.2008.02.011, 2008.

Eliazar, I. and Sokolov, I.: Gini characterization of extreme-value statistics, Phys. A-statistical Mech. Its Appl. - Phys. A, 389, 4462–4472, https://doi.org/10.1016/j.physa.2010.07.005, 2010.

Embrechts, P., Klüppelberg, C., and Mikosch, T.: Modelling extreme events for insurance and finance, Springer Berlin Heidelberg, 1997.

Fiorentino, M., Manfreda, S., and Iacobellis, V.: Peak runoff contributing area as hydrological signature of the probability distribution of floods, Adv. Water Resour., 30, 2123–2134, https://doi.org/10.1016/j.advwatres.2006.11.017, 2007.

Fischer, S. and Schumann, A.: Robust flood statistics: comparison of peak over threshold approaches based on monthly maxima and TL-moments, Hydrol. Sci. J., 61, 457–470, https://doi.org/10.1080/02626667.2015.1054391, 2016.

Gioia, A., Iacobellis, V., Manfreda, S., and Fiorentino, M.: Influence of infiltration and soil storage capacity on the skewness of the annual maximum flood peaks in a theoretically derived distribution, Hydrol. Earth Syst. Sci., 937–951, https://doi.org/10.5194/hess-16-937-2012, 2012.

Godrèche, C., Majumdar, S. N., and Schehr, G.: Statistics of the longest interval in renewal processes, J. Stat. Mech. Theory Exp., 2015, https://doi.org/10.1088/1742-5468/2015/03/P03014, 2015.

Hu, L., Nikolopoulos, E. I., Marra, F., and N., A. E.: Toward an improved estimation of flood frequency statistics from simulated flows, J. Flood Risk Manag., 1–13, https://doi.org/10.1111/jfr3.12891, 2023.

Jachens, E. R., Rupp, D. E., Roques, C., and Selker, J. S.: Recession analysis revisited: Impacts of climate on parameter estimation, Hydrol. Earth Syst. Sci., 24, 1159–1170, https://doi.org/10.5194/hess-24-1159-2020, 2020.

Kumar, M., Sharif, M., and Ahmed, S.: Flood estimation at Hathnikund Barrage, River Yamuna, India using the Peak-Over-Threshold method, ISH J. Hydraul. Eng., 26, 291–300, https://doi.org/10.1080/09715010.2018.1485119, 2020.

Laio, F., Porporato, A., Fernandez-Illescas, C. P., and Rodriguez-Iturbe, I.: Plants in water-controlled ecosystems: Active role in hydrologic processes and responce to water stress IV. Discussion of real cases, Adv. Water Resour., 24, 745–762, https://doi.org/10.1016/S0309-1708(01)00007-0, 2001.

https://doi.org/10.5194/egusphere-2023-660
Preprint. Discussion started: 2 May 2023

Lang, M., Ouarda, T. B. M. J., and Bobée, B.: Towards operational guidelines for over-threshold modeling, J. Hydrol., 225, 103–117, https://doi.org/10.1016/S0022-1694(99)00167-5, 1999.

Lehner, B., Liermann, C. R., Revenga, C., Vörömsmarty, C., Fekete, B., Crouzet, P., Döll, P., Endejan, M., Frenken, K., Magome, J., Nilsson, C., Robertson, J. C., Rödel, R., Sindorf, N., and Wisser, D.: High-resolution mapping of the world's reservoirs and dams for sustainable river-flow management, Front. Ecol. Environ., 9, 494–502, https://doi.org/10.1890/100125, 2011.

Lins, H. F.: Challenges to hydrological observations, WMO Bull., 57, 55–58, 2008.

Lombardo, F., Napolitano, F., Russo, F., and Koutsoyiannis, D.: On the Exact Distribution of Correlated Extremes in Hydrology, Water Resour. Res., 55, 10405–10423, https://doi.org/10.1029/2019WR025547, 2019.

Lu, P., Smith, J. A., and Lin, N.: Spatial characterization of flood magnitudes over the drainage network of the Delaware river basin, J. Hydrometeorol., 18, 957–976, https://doi.org/10.1175/JHM-D-16-0071.1, 2017.

Malamud, B. D. and Turcotte, D. L.: The applicability of power-law frequency statistics to floods, J. Hydrol., 322, 168–180, https://doi.org/10.1016/j.jhydrol.2005.02.032, 2006.

Marani, M. and Ignaccolo, M.: A metastatistical approach to rainfall extremes, Adv. Water Resour., 79, 121–126, https://doi.org/10.1016/j.advwatres.2015.03.001, 2015.

Marra, F., Nikolopoulos, E. I., Anagnostou, E. N., and Morin, E.: Metastatistical Extreme Value analysis of hourly rainfall from short records: Estimation of high quantiles and impact of measurement errors, Adv. Water Resour., 117, 27–39, https://doi.org/10.1016/j.advwatres.2018.05.001, 2018.

McDermott, T. K. J.: Global exposure to flood risk and poverty, Nat. Commun., 13, 6–8, https://doi.org/10.1038/s41467-022-30725-6, 2022.

Mejía, A., Daly, E., Rossel, F., Javanovic, T., and Gironás, J.: A stochastic model of streamflow for urbanized basins, Water Resour. Res., 50, 1984–2001, https://doi.org/10.1002/2013WR014834, 2014.

Merz, B., Basso, S., Fischer, S., Lun, D., Blöschl, G., Merz, R., Guse, B., Viglione, A., Vorogushyn, S., Macdonald, E., Wietzke, L., and Schumann, A.: Understanding heavy tails of flood peak distributions, Water Resour. Res., 1–37, https://doi.org/10.1029/2021wr030506, 2022.

Merz, B., Blöschl, G., Vorogushyn, S., Dottori, F., Aerts, J. C. J. H., Bates, P., Bertola, M., Kemter, M., Kreibich, H., Lall, U., and Macdonald, E.: Causes, impacts and patterns of disastrous river floods, Nat. Rev. Earth Environ., 2, 592–609, https://doi.org/10.1038/s43017-021-00195-3, 2021.

https://doi.org/10.5194/egusphere-2023-660
Preprint. Discussion started: 2 May 2023

Miniussi, A. and Marani, M.: Estimation of Daily Rainfall Extremes Through the Metastatistical Extreme Value Distribution: Uncertainty Minimization and Implications for Trend Detection, Water Resour. Res., 56, 1–18, https://doi.org/10.1029/2019WR026535, 2020.

Miniussi, A., Marani, M., and Villarini, G.: Metastatistical Extreme Value Distribution applied to floods across the continental United States, Adv. Water Resour., 136, 103498, https://doi.org/10.1016/j.advwatres.2019.103498, 2020.

Morrison, J. E. and Smith, J. A.: Stochastic modeling of flood peaks using the generalized extreme value distribution, Water Resour. Res., 38, 41-1-41–12, https://doi.org/10.1029/2001wr000502, 2002.

Müller, M. F., Dralle, D. N., and Thompson, S. E.: Analytical model for flow duration curves in seasonally dry climates, Water Resour. Res., 50, 5510–5531, https://doi.org/10.1002/2014WR015301, 2014.

Müller, M. F., Roche, K. R., and Dralle, D. N.: Catchment processes can amplify the effect of increasing rainfall variability, Environ. Res. Lett., 16, https://doi.org/10.1088/1748-9326/ac153e, 2021.

Mushtaq, S., Miniussi, A., Merz, R., and Basso, S.: Reliable estimation of high floods: A method to select the most suitable ordinary distribution in the Metastatistical extreme value framework, Adv. Water Resour., 161, 104127, https://doi.org/10.1016/j.advwatres.2022.104127, 2022.

Nerantzaki, S. D. and Papalexiou, S. M.: Tails of extremes: Advancing a graphical method and harnessing big data to assess precipitation extremes, Adv. Water Resour., 134, https://doi.org/10.1016/j.advwatres.2019.103448, 2019.

Pan, X., Rahman, A., Haddad, K., and Ouarda, T. B. M. J.: Peaks-over-threshold model in flood frequency analysis: a scoping review, Stoch. Environ. Res. Risk Assess., 36, 2419–2435, https://doi.org/10.1007/s00477-022-02174-6, 2022.

Papalexiou, S. M., Koutsoyiannis, D., and Makropoulos, C.: How extreme is extreme? An assessment of daily rainfall distribution tails, Hydrol. Earth Syst. Sci., 17, 851–862, https://doi.org/10.5194/hess-17-851-2013, 2013.

Papalexiou, S. M. and Koutsoyiannis, D.: Battle of extreme value distributions : A global survey on extreme daily rainfall, Water Resour. Res., 49, 187–201, https://doi.org/10.1029/2012WR012557, 2013.

Porporato, A., Daly, E., and Rodriguez-Iturbe, I.: Soil water balance and ecosystem response to climate change, Am. Nat., 164, 625–632, https://doi.org/10.1086/424970, 2004.

Pumo, D., Viola, F., La Loggia, G., and Noto, L. V.: Annual flow duration curves assessment in ephemeral small basins, J. Hydrol., 519, 258–270, https://doi.org/10.1016/j.jhydrol.2014.07.024, 2014.

Rajah, K., O'Leary, T., Turner, A., Petrakis, G., Leonard, M., and Westra, S.: Changes to the temporal distribution of daily precipitation, Geophys. Res. Lett., 41, 8887–8894, https://doi.org/10.1002/2014GL062156, 2014.

555 Rentschler, J., Salhab, M., and Jafino, B. A.: Flood exposure and poverty in 188 countries, Nat. Commun., 13, 3527, https://doi.org/10.1038/s41467-022-30727-4, 2022.

Resnick, S. I.: Heavy-Tail Phenomena: Probabilistic and Statistical Modeling, Springer US, New York, 2007.

Rogger, M., Pirkl, H., Viglione, A., Komma, J., Kohl, B., Kirnbauer, R., and Merz, R.: Step changes in the flood frequency curve : Process controls, Water Resour. Res., 48, 1–15, https://doi.org/10.1029/2011WR011187, 2012.

560 Santos, A. C., Portela, M. M., Rinaldo, A., and Schaefli, B.: Analytical flow duration curves for summer streamflow in Switzerland, Hydrol. Earth Syst. Sci., 22, 2377–2389, https://doi.org/10.5194/hess-22-2377-2018, 2018.

Sartori, M. and Schiavo, S.: Connected we stand: A network perspective on trade and global food security, Food Policy, 57, 114–127, https://doi.org/https://doi.org/10.1016/j.foodpol.2015.10.004, 2015.

Schaefli, B., Rinaldo, A., and Botter, G.: Analytic probability distributions for snow-dominated streamflow, Water Resour.
565 Res., 49, 2701–2713, https://doi.org/10.1002/wrcr.20234, 2013.

Seckin, N., Haktanir, T., and Yurtal, R.: Flood frequency analysis of Turkey using L-moments method, Hydrol. Process., 25, 3499–3505, https://doi.org/10.1002/hyp.8077, 2011.

Smith, J. A., Cox, A. A., Baeck, M. L., Yang, L., and Bates, P.: Strange Floods: The Upper Tail of Flood Peaks in the United States, Water Resour. Res., 54, 6510–6542, https://doi.org/10.1029/2018WR022539, 2018.

570 Spearman, C.: The proof and measurement of association between two things, Am. J. Psychol., 15, 72–101, https://doi.org/10.2307/1412159, 1904.

Székely, G. J., Rizzo, M. L., and Bakirov, N. K.: Measuring and testing dependence by correlation of distances, Ann. Stat., 35, 2769–2794, https://doi.org/10.1214/009053607000000505, 2007.

Tarasova, L., Basso, S., and Merz, R.: Transformation of Generation Processes From Small Runoff Events to Large Floods,
575 Geophys. Res. Lett., 47, https://doi.org/10.1029/2020GL090547, 2020.

Tarasova, L., Basso, S., Zink, M., and Merz, R.: Exploring Controls on Rainfall-Runoff Events: 1. Time Series-Based Event Separation and Temporal Dynamics of Event Runoff Response in Germany, Water Resour. Res., 54, 7711–7732, https://doi.org/10.1029/2018WR022587, 2018.

Tashie, A., Pavelsky, T., and Band, L. E.: An Empirical Reevaluation of Streamflow Recession Analysis at the Continental
580 Scale, Water Resour. Res., 56, 1–18, https://doi.org/10.1029/2019WR025448, 2020a.

Tashie, A., Pavelsky, T., and Emanuel, R. E.: Spatial and Temporal Patterns in Baseflow Recession in the Continental United States, Water Resour. Res., 56, 1–18, https://doi.org/10.1029/2019WR026425, 2020b.

https://doi.org/10.5194/egusphere-2023-660
Preprint. Discussion started: 2 May 2023

Vázquez, A., Oliveira, J. G., Dezsö, Z., Goh, K. Il, Kondor, I., and Barabási, A. L.: Modeling bursts and heavy tails in human dynamics, Phys. Rev. E - Stat. Nonlinear, Soft Matter Phys., 73, 1–19, https://doi.org/10.1103/PhysRevE.73.036127, 2006.

Villarini, G. and Smith, J. A.: Flood peak distributions for the eastern United States, Water Resour. Res., 46, 1–17, https://doi.org/10.1029/2009WR008395, 2010.

Villarini, G., Smith, J. A., Baeck, M. L., Marchok, T., and Vecchi, G. A.: Characterization of rainfall distribution and flooding associated with U.S. landfalling tropical cyclones: Analyses of Hurricanes Frances, Ivan, and Jeanne (2004), J. Geophys. Res. Atmos., 116, https://doi.org/10.1029/2011JD016175, 2011.

Volpi, E., Fiori, A., Grimaldi, S., Lombardo, F., and Koutsoyiannis, D.: Save hydrological observations! Return period estimation without data decimation, J. Hydrol., 571, 782–792, https://doi.org/10.1016/j.jhydrol.2019.02.017, 2019.

Wang, H., Merz, R., Yang, S., Tarasova, L., and Basso, S.: Emergence of heavy tails in streamflow distributions: the role of spatial rainfall variability, Adv. Water Resour. J., 171, https://doi.org/10.1016/j.advwatres.2022.104359, 2022.

Wietzke, L. M., Merz, B., Gerlitz, L., Kreibich, H., Guse, B., Castellarin, A., and Vorogushyn, S.: Comparative analysis of scalar upper tail indicators, Hydrol. Sci. J., 65, 1625–1639, https://doi.org/10.1080/02626667.2020.1769104, 2020.

Wilson, P. S. and Toumi, R.: A fundamental probability distribution for heavy rainfall, Geophys. Res. Lett., 32, 1–4, https://doi.org/10.1029/2005GL022465, 2005.

Wittenberg, H.: Baseflow recession and recharge as nonlinear storage processes, 726, 715–726, 1999.